Bevacizumab dosing strategy in paediatric cancer patients based on population pharmacokinetic analysis with external validation

Kelong Han,[1] Thomas Peyret,[2] Angelica Quartino,[1] Nathalie H. Gosselin,[2] Sridharan Gururangan,[3] Michela Casanova,[4] Johannes H. M. Merks,[5] Maura Massimino,[4] Jacques Grill,[6] Najat C. Daw,[7] Fariba Navid,[8] Jin Jin[1] & David E. Allison[1]

[1]Clinical Pharmacology, Genentech Inc., South San Francisco, CA, USA, [2]Pharsight Consulting Services, Montreal, QC, Canada, [3]Preston Robert Tisch Brain Tumor Center, Duke University Medical Center, Durham, NC, [4]Pediatric Oncology Unit, Fondazione IRCCS Istituto Nazionale dei Tumori, Milano, Italy, [5]Department of Pediatric Oncology, Emma Children's Hospital-Academic Medical Center (EKZ-AMC), Amsterdam, The Netherlands, [6]Gustave Roussy, Faculté de Médecine, University Paris-SUD, Villejuif, France, [7]Division of Pediatrics, MD Anderson Cancer Center, Houston, TX and [8]Department of Oncology, St Jude Children's Research Hospital, Memphis, TN, USA

WHAT IS ALREADY KNOWN ABOUT THIS SUBJECT

- Bevacizumab pharmacokinetics and dosing guidelines have not been comprehensively investigated in paediatric patients.
- Multiple strategies are currently used for dosing therapeutic antibodies in children.
- Given the similarity in pharmacokinetics among many monoclonal antibodies, developing appropriate and practical paediatric dosing guidelines for bevacizumab may inform other therapeutic antibodies.

AIM

The aim of the present study was to evaluate the pharmacokinetics of bevacizumab and various dosing strategies for this agent in paediatric patients.

METHODS

Data were collected from 232 paediatric patients (1971 concentrations) in five studies, with a wide range of age (0.5 – 21 years), body weight (BWT; 5.9 – 125 kg), and regimens (5 – 15 mg kg^{-1} biweekly or triweekly). Data from 152 patients (1427 concentrations) and 80 patients (544 concentrations) were used for model building and external validation, respectively. Steady-state exposure was simulated under BWT-based, body surface area (BSA)-based, ideal body weight (IBW)-based, and tier-based doses. NONMEM and R were used for analyses.

RESULTS

Typical estimates of clearance, central volume of distribution (V1), and median half-life were 9.04 ml h^{-1}, 2851 ml, and 19.6 days, respectively. Clearance decreased with increasing albumin. Clearance and V1 increased with BWT and were higher in male patients. Clearance and V1 were lower in children with primary central nervous system (CNS) tumours than in children with sarcomas, resulting in 49% higher trough (Cmin) and 29% higher peak (Cmax) concentrations. BWT-adjusted clearance and V1 remained unchanged across ages. Paediatric Cmin was similar to adult Cmin under all dosing strategies. Paediatric Cmax exceeded adult Cmax under tier-based doses.

WHAT THIS STUDY ADDS

- Bevacizumab pharmacokinetics is similar between paediatric and adult patients and remains unchanged across ages in children.
- Bevacizumab exposure was higher in children with primary CNS tumours than in children with sarcomas.
- BSA-based, IBW-based, and tier-based doses offered no substantial advantage over the BWT-based dose that is currently used for bevacizumab in adults.

CONCLUSIONS

BWT-adjusted pharmacokinetic parameter estimates in paediatric patients were similar to those in adults, and similar across ages. Bevacizumab exposure was higher in children with primary CNS tumours than in children with sarcomas. BSA-based, IBW-based, and tier-based doses offered no substantial advantage over the BWT-based dose currently used in adults for bevacizumab. Given the similarity in pharmacokinetics among many monoclonal antibodies, this may help to develop practical paediatric dosing guidelines for other therapeutic antibodies.

Introduction

Bevacizumab (Avastin®, Genentech Inc., South San Francisco, CA, USA) is a humanized monoclonal immunoglobulin G (IgG) 1 antibody that specifically binds to, and neutralizes the biological activity of, vascular endothelial growth factor A (VEGF-A), a key isoform of VEGF involved in angiogenesis, and a well-characterized pro-angiogenic factor [1]. Bevacizumab causes inhibition of tumour angiogenesis by blocking VEGF-A from binding to its receptors and leads to tumour growth inhibition. Bevacizumab in combination with standard therapy has received marketing authorization for use in the treatment of various cancers, including metastatic colorectal cancer [2, 3], non-small-cell lung cancer [4], breast cancer [5], renal cell carcinoma [6], cervical cancer [7], and ovarian cancer [8].

Appropriate and practical dosing guidelines of monoclonal antibody drugs (mAbs) in paediatric cancer patients are still not clearly defined. Currently, there are mainly two types of dosing strategies for mAbs in children: tier-based (a fixed dose for the approved age or body size range) and body size based (linear dose scaling by body size) [9]. For body size-based dosing, total body weight (BWT) is currently the most widely used body size metric. Body surface area (BSA) was proposed to be a more satisfactory index of drug requirements than BWT or age, particularly during infancy and childhood [10]. Ideal body weight (IBW) has also been used for dosing paediatric patients [11].

Population pharmacokinetic (PK) modelling is a powerful tool for determining the most appropriate and practical dosing strategies. The population PK of bevacizumab was previously characterized in adults [12], and the model was updated (Supplementary Table S1). In adult cancer patients, clearance (CL) and central volume of distribution (V1) increased with BWT, decreased with albumin, and were lower in females. In addition, CL decreased with total protein, and V1 increased with tumour burden.

However, bevacizumab PK and dosing guidelines have not been comprehensively evaluated in paediatric cancer patients, especially very young patients under 3 years of age. Only two previous studies evaluated bevacizumab PK in, 10 and 27 patients between the ages of 7 years and 21 years, respectively [13, 14]. The limited data on bevacizumab PK to inform dosing guidelines in paediatric cancer patients have mainly been derived from the many challenges in conducting paediatric studies, including limited access to the population of interest, low consent rates, etcetera.

Five dedicated paediatric clinical studies have been conducted and included evaluation of bevacizumab PK (Table 1): a Phase I study AVF2771s (NCT00085111) [13] and four Phase II studies AVF4117s (NCT00667342) [14], AVF3842s (NCT00381797) [15], BO20924 (NCT00643565), and BO25041 (NCT01390948). These allowed for the opportunity to investigate bevacizumab PK in paediatric cancer patients over a wide range of age, body size, cancer types, and dosing regimens. The objectives of the current analysis were to develop a robust population PK model in paediatric cancer patients and develop the most appropriate and practical dosing strategy.

Methods

Patients

Patients with at least one PK sample were included in the analysis. Serum bevacizumab concentrations were determined at Genentech, Inc. using an enzyme-linked immunosorbent assay that used recombinant human VEGF for capture and a goat antibody to human IgG conjugated to horseradish peroxidase for detection. The lowest limit of quantification (LLOQ) was 78 ng ml^{-1} in serum [13]. Concentrations below the LLOQ were omitted.

The clinically relevant covariates tested included those related to demographics, biochemical tests, concomitant medications, and pathophysiological factors (Table 1). The

Table 1

Summary of studies and patient characteristics

	Model building population N = 152	External validation population N = 80
PK samples*	1427 (1592)	544 (554)
Study	1. AVF2771s††: Refractory sarcomas	1. BO25041: Primary CNS tumours
	2. AVF3842s: Primary CNS tumours	2. BO20924 (remaining data): Metastatic soft-tissue sarcoma
	3. AVF4117s: Newly diagnosed osteosarcoma	
	4. BO20924 (interim data): Metastatic soft-tissue sarcoma	
Dosing regimen†	Q2W: 5, 10, 15 mg kg^{-1} Q3W: 7.5, 15 mg kg^{-1}	Q2W: 10 mg kg^{-1} Q3W: 7.5 mg kg^{-1}
Infants‡	7	2
Age $<$ 3 years§	9	3
Age ¶ (year)	n = 152	n = 80
	10.8 (44.1)	10.4 (42.0)
	10.8 [0.5–21.0]	11.0 [1.4–17.6]
BSA ¶ (m^2)	n = 142	n = 80
	1.26 (35.1)	1.24 (31.9)
	1.30 [0.32–2.39]	1.28 [0.50–2.05]
Body weight ¶ (kg)	n = 152	n = 80
	43.6 (52.5)	40.3 (46.6)
	43.8 [5.94–125.0]	40.0 [11.8–82.3]
Albumin ¶ (g l^{-1})	n = 98	n = 80
	38.8 (13.9)	38.7 (15.0)
	39.0 [24.0–52.0]	39.0 [23.0–51.0]
Total protein ¶ (g l^{-1})	n = 99	n = 32
	69.3 (10.7)	67.3 (10.5)
	70.0 [51.0–87.0]	67.0 [56.0–82.0]
Gender F:M**	70 (46.1%): 82 (53.9%)	30 (37.5%): 50 (62.5%)

BSA, body surface area; CNS, central nervous system; CV, coefficient of variation; N, total number of patients in this study; n, number of patients with available information about this variable; PK, pharmacokinetic; Q2W, once every 2 weeks; Q3W, once every 3 weeks. *Displayed as number of PK samples included in the analysis (total number of PK samples collected). †bevacizumab was given via an intravenous infusion over 30–90 minutes. ‡Infants are defined as children between 0 and 2 years of age, according to the Food and Drug Administration guidance [28]. §Number of patients below 3 years of age. ¶Displayed as: number of patients with available data; mean (CV%); median [minimum – maximum]. **F (female):M (male), displayed as number of patients (percentage). ††bevacizumab was given as single-agent escalating dose in AVF2771s and in combination with chemotherapy in all other studies.

missing value was imputed as the median for continuous covariates or the most frequent value for categorical covariates derived with available data for each gender.

Population PK modelling

A population PK model was developed using data (Table 1) from studies AVF2771s, AVF3842s, AVF4117s, and BO20924 (interim data). Nonlinear mixed-effects modelling was performed using NONMEM (version 7.2; ICON Development Solutions, Ellicott City, MD, USA) [16] using the FOCE (first-order conditional estimation method) method of estimation with interaction, Perl-speaks-NONMEM (version 3.5.3; Uppsala University, Uppsala, Sweden) [17] and R 3.0.3 [18]. Several models were tested to select the optimal base model. The base model included a power function of body size (e.g. BWT) on all PK parameters:

$$P_i = P_{TV} \times \left(\frac{BWT_i}{70}\right)^{\theta_P}$$

where BWT_i = baseline BWT of patient i; P_i = typical PK parameters of patients with BWT_i; P_{TV} = typical value

of PK parameters for patients with a BWT of 70 kg; θ_P = exponent for the PK parameter P.

The base model was evaluated using either theoretical (0.75 for CLs; 1 for volumes of distribution) [19] or fitted values of exponent θ_P. The nonlinearity of the PK was assessed using the Michaelis–Menten model.

The quality of fit was evaluated using a standard model discrimination process including statistical criteria [i.e. minimum of objective function value (OFV)], adequate estimation of the parameters (e.g. relative standard error $<$ 50%), and graphical representations of goodness-of-fit. The final model was established in a stepwise manner by forward addition followed by backward elimination, with a significance level of $P < 0.05$ and $P < 0.001$ (OFV decrease of 3.84 and 10.83 for one degree of freedom), respectively.

The effect of n covariates on PK parameters was coded using a multiplicative model:

$$\theta_i = \theta_{TV} \times Effect_{1,i} \times \ldots \times Effect_{n,i}$$

where θ_i is the typical value of the parameter for patients with a set of covariates i, θ_{TV} is the typical value

of the PK parameter for patients having the covariate values equal to the median of the covariate for all patients, and $Effect_{1,i}$ through $Effect_{n,i}$ are multiplicative factors of the effects for covariate 1 through n, for the set of covariates i.

The multiplicative factor was defined using the power function for continuous covariates:

$$Effect_i = \left(\frac{Cov_i}{Cov_{reference\ value}}\right)^{\theta_{eff}}$$

and defined as follows for categorical covariates:

if this categorical covariate is equal to 0, then $Effect_i = 1$
if this categorical covariate is not equal to 0,

$$\text{then}\ \ Effect_i = e^{ln(\theta_{eff})}$$

where $Effect_i$ is the multiplicative factor of the covariate effect for covariate i, Cov_i is the covariate value, $Cov_{reference\ value}$ is the median of the covariate for all patients and $ln(\theta_{eff})$ is the exponent of the power function to be estimated. $ln(\theta_{eff})$ was used to avoid bounds during the calculation by NONMEM.

Model evaluation and sensitivity analysis

The population PK models were evaluated using diagnostic plots [20, 21], visual predictive check (VPC) [21, 22], prediction-corrected VPC (pcVPC) [23], bootstrapping [24] and shrinkage assessment [25]. VPC, pcVPC, and bootstrapping were all performed using 1000 replicates based on the final model. The relative impact of each covariate included in the final model alone on PK parameters and exposure was explored. Exposure, including steady-state trough (Cmin) and peak (Cmax) concentrations, was computed given a dose of bevacizumab of 10 mg kg^{-1} once every two weeks (Q2W) using the final model.

External validation

After the final model was built, data from study BO25041 and the remaining data from BO20924 (Table 1) became available and subsequently were used to validate the model externally. Predicted concentrations (C_{PRED}) for the validation population were obtained using *post hoc* Bayesian forecasting by fixing the parameters in the structural and variance models to the final estimates. Prediction errors (PE) were calculated for each concentration as PE = ($C_{OBS} - C_{PRED}$)/C_{PRED}, where C_{OBS} denotes observed concentrations. pcVPC was used to compare the 95% prediction interval (PI) and C_{OBS}.

Predicted PK parameters (P_{PRED}) for each patient were obtained based on individual covariate values using the equations in the final model without considering observed concentrations. *Post hoc* estimates of PK parameters (P_{EST}) were obtained based on observed concentrations and the final model. PE were calculated as ($P_{EST} - P_{PRED}$)/P_{PRED}.

Evaluation of dosing strategies

Bevacizumab steady-state Cmin and Cmax in paediatric patients were simulated under the four most widely discussed dosing strategies: BWT-, BSA-, IBW-, and tier-based doses, which were compared to Cmin and Cmax simulated in adult patients receiving 10 mg kg^{-1} Q2W. The IBW of each patient was calculated by multiplying the square of the height (m^2) by body mass index (BMI), which was determined using the 50th percentile of the gender-specific BMI-for-age growth charts published by the Center for Disease Control and Prevention [26]. The paediatric doses (Q2W) used in the simulation were determined so that the simulated paediatric steady-state area under the curve (AUC) matched the simulated adult steady-state AUC. The final doses used in the simulation were 10 mg kg^{-1} for the BWT-based dose, 398 mg m^{-2} for the BSA-based dose, 11 mg kg^{-1} for the IBW-based dose, and as follows for the tier-based dose: 180 mg for <15 kg; 360 mg for 15–40 kg; 640 mg for >40 kg. The 90% PI was generated by simulating 1000 times using the base model of paediatric and adult patients (Supplementary Table S1). The individual Cmin and Cmax of the 152 paediatric patients were also simulated using the individual *post hoc* PK parameter estimates. In order to compare to the bevacizumab maximum tolerated dose (MTD) of 15 mg kg^{-1} previously determined in adults [27], the BSA-, IBW-, and tier-based doses of each individual paediatric patient were converted to mg kg^{-1} dose by dividing the actual dose by BWT.

Results

Patients

A total of 2146 bevacizumab serum concentrations from 232 patients were collected and underwent bioanalysis. Of these, 138 concentrations were below the LLOQ (prestudy samples) and 37 were outliers (mainly due to human errors in recording time and dose). Information about studies and patient characteristics is summarized in Table 1. All patient characteristics were similar between children with primary central nervous system (CNS) tumours (AVF3842s and BO25041) and children with sarcomas (AVF2771s, AVF4117s, and BO20924). The percentage of children with primary CNS tumours with albumin below normal level (35 g l^{-1}) appeared lower than that of children with sarcomas: 8% *vs.* 24%. Noticeably, nine infants (as defined by the US Food and Drug Administration guidance [28]) were included in the analysis. Albumin and total protein levels in paediatric patients were comparable to those in adults.

Population PK modelling

Out of the 232 paediatric patients, data from 152 patients (1427 concentrations) were used for model building. The optimal base model was a linear two-compartment model with theoretical exponents fixed at 0.75 for CL and inter-compartment clearance (Q), and estimated for V1 and peripheral volume of distribution (V2), full-block inter-individual variability (IIV) on CL, V1, and V2 with combined additive and proportional residual error. The Michaelis–Menten model did not significantly ($P > 0.05$) improve the model fitting based on the range of available concentrations (0.4 – 741 µg ml^{-1}). The estimates of typical bevacizumab CL, V1, Q, V2, and median terminal half-life values were 3.05 ml day^{-1} kg^{-1}, 40.0 ml kg^{-1}, 9.34 ml day^{-1} kg^{-1}, 34.6 ml kg^{-1}, and 19.6 days, respectively, in paediatric cancer patients, similar to values in adults of 3.00 ml day^{-1} kg^{-1}, 39.1 ml kg^{-1}, 7.57 ml day^{-1} kg^{-1}, 40.7 ml kg^{-1} and 20 days, respectively (Supplementary Table S1). The correlation between V1 and albumin was not significant in the final model. After taking into account BWT, CL and V1 still decreased with increasing albumin, and were higher in male patients (Supplementary Figure S1), but were no longer correlated with age (Figure 1).
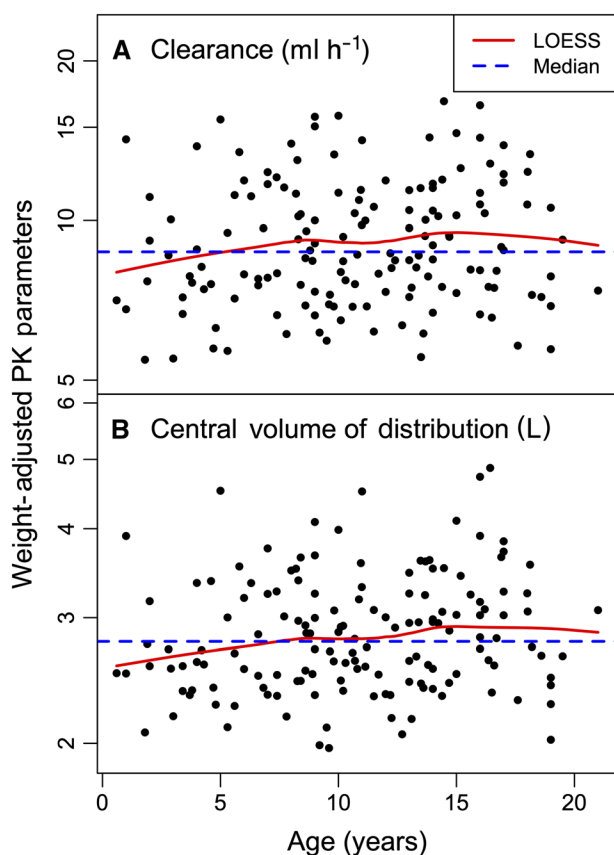
Bevacizumab CL and V1 in children with primary CNS tumours ($n = 76$) were significantly ($P < 0.0001$) lower than in children with sarcomas ($n = 76$). This effect was first indicated by the difference in CL and V1 across the four studies (Supplementary Figure S1). Models with all possible combinations of study effect on CL and V1 were compared one by one. In the resulting final model, CL and V1 in AVF2771s, AVF4117s, and AVF3842s (various sarcomas) were not statistically significantly different from each other, but were statistically significantly different from those in AVF3842s (primary CNS tumours).

Parameter estimates of the final model are summarized in Table 2. Bevacizumab CL and V1 for a paediatric patient i were described as follows:

$$CL_i = 9.90 \times \left(\frac{BWT_i}{70}\right)^{0.75} \times \left(\frac{ALBU_i}{39}\right)^{-0.3}$$

$$\times 1.11 \text{ (if male)} \times 0.725 \text{ (if primary CNS tumours)}$$

$$V1_i = 2850 \times \left(\frac{BWT_i}{70}\right)^{0.701}$$

$$\times 1.14 \text{ (if male)} \times 0.854 \text{ (if primary CNS tumours)}$$

Model evaluation and sensitivity analysis

Goodness-of-fit plots showed good agreement between predicted and observed bevacizumab concentrations, with no apparent bias in residual (Supplementary Figure S2). Shrinkage on all parameters and IIV was <20%. The pcVPC result (Figure 2) showed that the 2.5th, 50th, and 97.5th percentiles of observed concentrations were within the predicted 95% confidence interval (CI) of these percentiles, suggesting accurate model fitting across a wide range of dosing regimens and time courses. Bootstrapping resulted in median parameter estimates and 95% CIs similar to the estimates from the original dataset, indicating that the final model provided good precision for parameter estimation.

The impact of the variation for a single covariate included in the final model on CL and V1 (data not shown) and steady-state exposure (Cmin and Cmax) were demonstrated by comparing the simulated CL, V1, and exposure of patients with extreme covariate values (5th and 95th percentiles) to a typical patient with a median covariate value (Figure 3). Among all covariates, BWT had the strongest impact on CL and V1. With BWT <24.1 kg, CL and V1 were reduced to less than 50% of the typical value. Primary CNS tumours had the second strongest impact on CL and V1. In children with primary CNS tumours, CL and V1 were 27% and 15% lower than the typical value, respectively. The gender effect on CL and V1 was less than 25%. The IIV area mostly covered ±50% variation of the individual CL and V1 values.

Figure 1

Weight-adjusted pharmacokinetic (PK) parameters. (A) Clearance and (B) central volume of distribution obtained from the bevacizumab base model across age. LOESS, locally weighted scatterplot smoothing

Table 2

Parameter estimates of the final model in paediatric cancer patients

| Parameters	Estimates	RSE (%)	95% CI	Bootstrapping median	Bootstrapping 95% CI	Shrinkage (%)
CL (ml h^{-1})	9.90	4.1	[9.10, 10.7]	9.90	[9.16, 10.7]	
V1 (ml)	2850	3.0	[2683, 3017]	2850	[2701, 3005]	
Q (ml h^{-1})	28.0	10.4	[22.3, 33.8]	28.2	[23.0, 35.4]	
V2 (ml)	2564	5.8	[2274, 2854]	2569	[2294, 2852]	
BWT on CL	0.75	Fixed		0.75	Fixed	
Male on CL	1.11	4.1	[1.02, 1.20]	1.11	[1.02, 1.20]	
ALBU on CL	−0.300	50.6	[−0.597, −0.00227]	−0.302	[−0.600, 0.0366]	
Primary CNS tumour on CL	0.725	4.3	[0.666, 0.789]	0.725	[0.667, 0.784]	
BWT on V1	0.701*	3.9*	[0.647, 0.755]*	0.701	Fixed	
Male on V1	1.14	3.5	[1.07,1.22]	1.14	[1.07, 1.22]	
Primary CNS tumour on V1	0.854	3.7	[0.793, 0.919]	0.853	[0.795, 0.918]	
BWT on Q	0.75	Fixed		0.75	Fixed	
BWT on V2	0.766*	14.4*	[0.550, 0.982]*	0.766	Fixed	
Prop. error (%)	13.9	6.9	[11.9, 15.7]	13.9	[12.0, 15.5]	10.4
Add. error (µg ml^{-1})	3.06	25.1	[0.406,4.30]	3.09	[1.43, 4.50]	10.4
IIV CL (%)	21.4	7.4	[18.0, 24.3]	21.1	[18.2, 24.2]	10.4
IIV V1 (%)	17.6	9.2	[14.0, 20.5]	17.3	[14.2, 20.4]	14.3
IIV V2 (%)	58.0	13.3	[40.1, 71.6]	57.3	[41.8, 71.4]	18.1
Var. IIVs CL and V1	0.0248	17.6	[0.0162, 0.0334]	0.0244	[0.0162, 0.0328]	
Var. IIVs CL and V2	0.0228	75.2	[−0.0108, 0.0563]	0.0216	[−0.0160, 0.0547]	
Var. IIVs V1 and V2	0.0248	51.0	[−6.56 × 10^{-6}, 0.0496]	0.0249	[0.000875, 0.0499]	

Add, additive; ALBU, baseline albumin; BWT, body weight; CI, confidence interval; CL, clearance (ml h^{-1}); CNS, central nervous system; IIV, inter-individual variability; Prop, proportional; Q, inter-compartment clearance; RSE, relative standard error; Var., variance; V1, central volume of distribution; V2, peripheral volume of distribution; *value estimated for the base model.
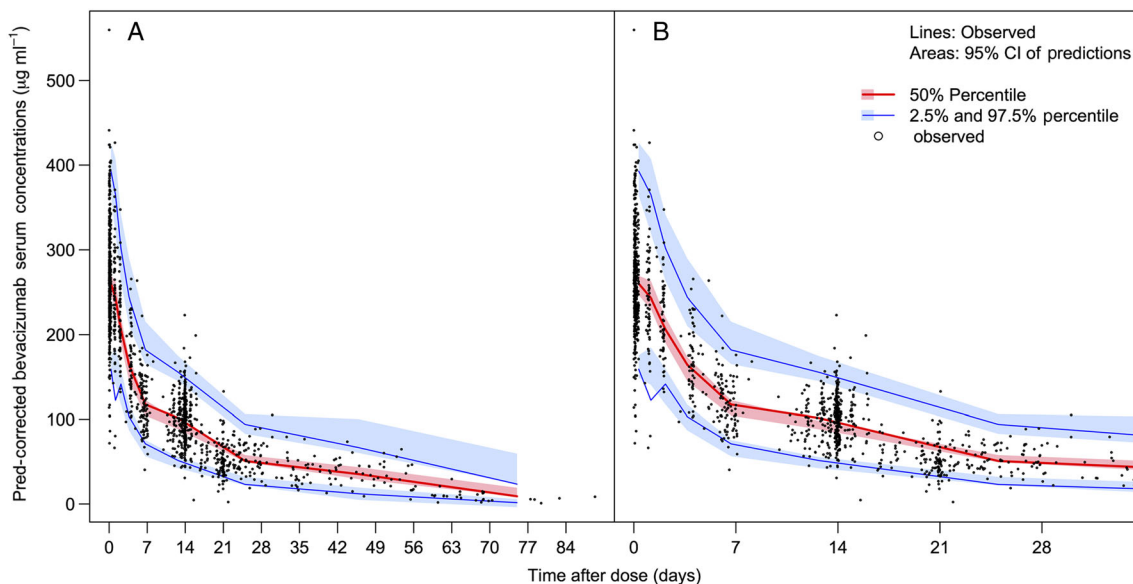
Figure 2

(A) Prediction-corrected visual predictive check for the serum concentration–time profiles of bevacizumab using the final model in paediatric cancer patients. (B) Section of (A) before day 35 after dose administration, where the majority (94%) of the data points lay. CI, confidence interval; Pred, population prediction

Primary CNS tumours had an almost equally strong impact as BWT on bevacizumab steady-state Cmin (Figure 3). Cmin and Cmax in children with primary CNS tumours were 49% and 29% higher than in children with sarcomas, respectively. Variations of exposure in paediatric cancer patients due to albumin and gender effect were less than 31% and 12%, respectively.
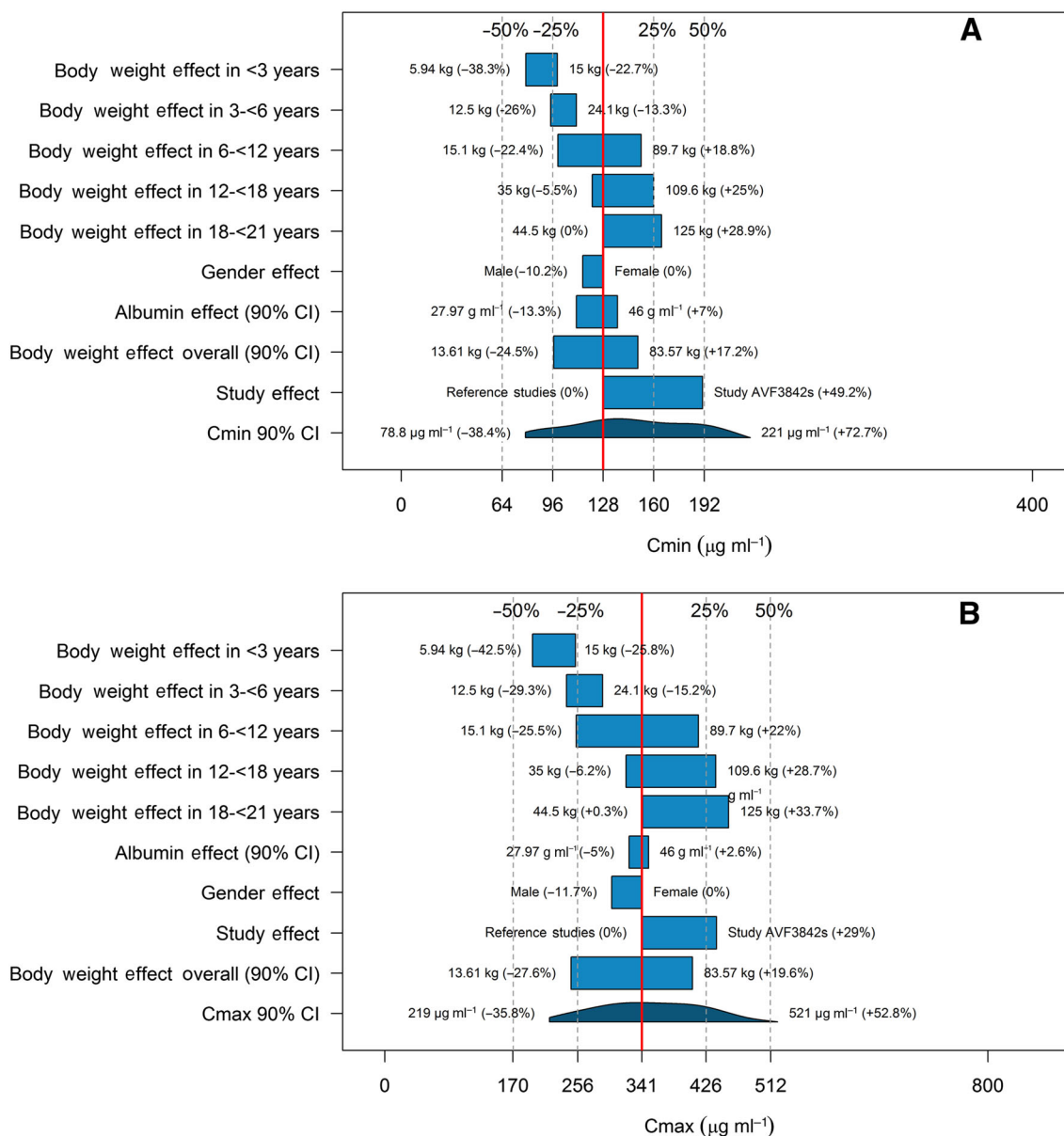
Figure 3

Impact of the variation for a single covariate included in the final model on steady-state bevacizumab exposure in paediatric cancer patients. (A) Trough concentration (Cmin) and (B) peak concentration (Cmax). Red vertical lines represent the 'base', defined as the exposure of a typical patient – i.e. a 44-kg female paediatric patient with an albumin level of 39 g l^{-1} and sarcomas. The dark blue-shaded curve at the bottom, with a value at each end, shows the 5th to 95th percentile exposure range across the entire population. Each light blue-shaded bar represents the influence of a single covariate on the steady-state exposure after repeated bevacizumab doses of 10 mg kg^{-1} once every two weeks. The label at left end of the bar represents the covariate being evaluated. The upper and lower values for each covariate capture 90% of the plausible range in the population. The length of each bar describes the potential impact of that particular covariate on bevacizumab steady-state exposure, with the percentage value in the parentheses at each end representing the percentage change in exposure from the 'base'. The most influential covariate is at the bottom of the plot for each exposure metric, except for the body weight effect stratified by age group, which is displayed on the top. CI, confidence interval; Cmax, peak concentration; Cmin, trough concentration
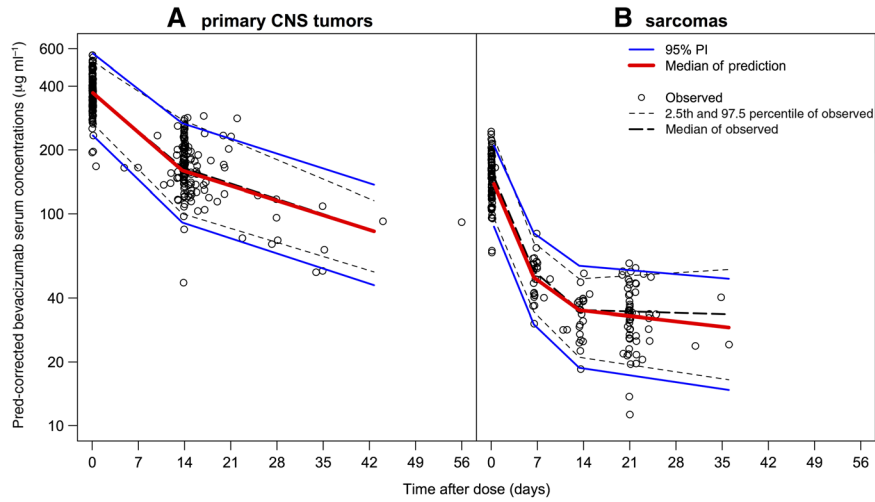
External validation

Out of the 232 paediatric patients, data from 80 patients (544 concentrations) were used for external validation (Table 1). Only 5.1% of prediction-corrected observations fell outside the 95% PI, which was very close to the 2.5th and 97.5th percentiles of observed concentrations (Figure 4). Mean PE for concentrations, CL, and V1 were 3.54%, −1.84%, and −0.06%, respectively.

No bias in PE was observed over time and across predicted values. In spite of the substantial difference in exposure between primary CNS tumours (Figure 4a) and sarcomas (Figure 4b), the model could predict both very well.

Evaluation of dosing strategies

Bevacizumab steady-state Cmin in paediatric patients generally fell within the 90% PI of Cmin in adult patients

Figure 4

External validation for (A) primary CNS tumours and (B) sarcomas. About 95% of the prediction-corrected observations fall between the 95% prediction interval boundaries, which are very close to the observed 2.5th and 97.5th percentiles. CNS, central nervous system; PI, prediction interval
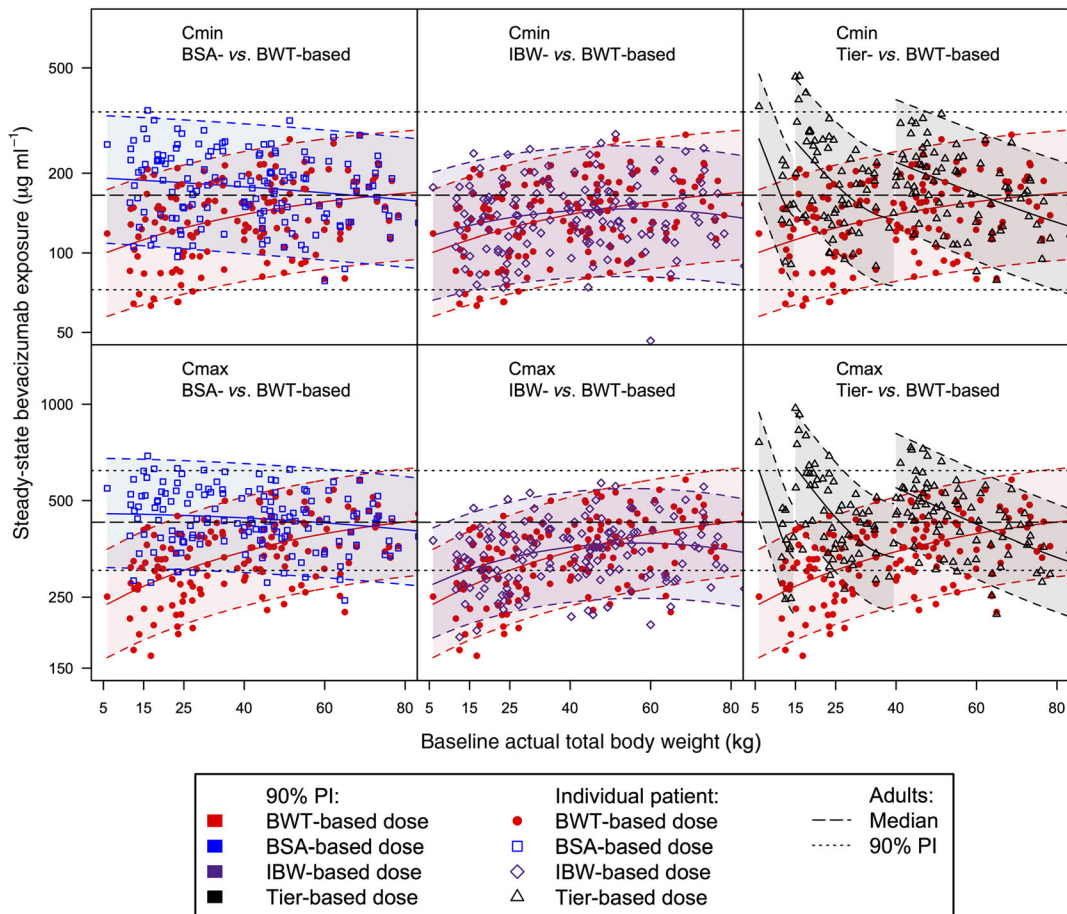
Figure 5

Simulated steady-state bevacizumab exposure in paediatric patients under BWT-, BSA-, IBW-, and tier-based doses. Equivalent doses (once every 2 weeks) were used: 10 mg kg^{-1} for the BWT-based dose, 398 mg m^{-2} for the BSA-based dose, and 11 mg kg^{-1} for the IBW-based dose. The tier-based dose in each BWT range was determined so that the steady-state area under the curve (AUC) under these doses matched the adult steady-state AUC: 180 mg for <15 kg, 360 mg for 15 – 40 kg, 640 mg for >40 kg. Only patients with a BWT below 80 kg are displayed. BSA, body surface area; BWT, total body weight; Cmax, peak concentration; Cmin, trough concentration; IBW, ideal body weight; PI, prediction interval

under all dosing strategies (Figure 5), meaning that Cmin in less than 5% of paediatric patients fell below the lower boundary or above the upper boundary of the 90% PI of Cmin in adult patients. Cmin and Cmax in paediatric patients increased under the BWT-based dose and decreased under the BSA-based dose with increasing BWT. Under the BWT-based dose, Cmax in approximately 33% of the paediatric patients fell below the lower boundary of the 90% PI of adult Cmax but did not exceed the upper boundary of the 90% PI of adult Cmax. Under the BSA-based dose, Cmax in paediatric patients generally fell within the 90% PI of adult Cmax. Under the tier-based dose, Cmax in approximately 12% of the paediatric patients exceeded the upper boundary of the 90% PI of adult Cmax. Cmin and Cmax in paediatric patients were similar between BWT- and IBW-based doses. When converted to an equivalent mg kg^{-1} dose, IBW-based doses appeared similar to BWT-based doses, whereas BSA- and tier-based doses increased with decreasing BWT and age (Supplementary Figure S3). The converted mg kg^{-1} doses corresponding to the BSA- and tier-based doses in young patients exceeded the bevacizumab MTD of 15 mg kg^{-1} previously determined in adults [27].

Discussion

The present analysis was a comprehensive evaluation of bevacizumab dosing strategies in paediatric cancer patients, including very young patients, by population PK modelling and simulations. We assembled a large paediatric PK population of 232 patients from five dedicated paediatric studies, with 12 patients under the age of 3 years. A robust population PK model was built and externally validated. We demonstrated that BSA-, IBW-, and tier-based dosing strategies offered no substantial advantage over the BWT-based dose that is currently used in adults for bevacizumab.

The population PK model developed was robust, as demonstrated by goodness-of-fit plots (Supplementary Figure S2), pcVPC (Figure 2), and external validation (Figure 4). In spite of the substantial difference in exposure between primary CNS tumours (Figure 4a) and sarcomas (Figure 4b), the model could predict both very well, confirming the robustness of the final model. Shrinkage was small for all PK parameters and IIV, suggesting that the PK data collected were sufficient to characterize the PK parameters and IIV.

Bevacizumab PK is similar between paediatric and adult cancer patients, as demonstrated by similar PK parameters after taking into account BWT. The median terminal half-life of 19.6 days (range 9–78 days) in paediatric cancer patients is also similar to that in adults (20 days). The low IIV of 21.4% and 17.6% observed for CL and V1, respectively, in paediatric patients is typical for antibody drugs. Nonlinear PK was not observed in paediatric patients, similar to the observation in adults. Nonlinear PK

and target-mediated disposition was not observed, probably because the bevacizumab molar concentration is thousands of times higher than that of the target VEGF-A [12], a soluble antigen [29].

There was a trend of unknown clinical significance toward lower CL and V1 in children with primary CNS tumours than in those with sarcomas: CL and V1 were 27% and 15% lower, respectively, resulting in a 49% higher Cmin and 29% higher Cmax at steady state (Figure 3). This trend could not be confirmed in adults because these two types of tumour are rare in adults. In addition, PK in adults with glioblastoma from the Avastin in Glioblastoma (AVAglio) trial (BO21990; NCT00943826) appeared similar to that in other types of solid tumour. However, this trend may not be clinically relevant, given that exposure in children with primary CNS tumours or sarcomas fell within the range of adult exposure (Figure 5). The number of children with primary CNS tumours ($n = 76$) and sarcomas ($n = 76$) in the model-building dataset was equal, and patient characteristics were similar (Table 1), with albumin being slightly higher in children with primary CNS tumours. The underlying mechanism is unclear but we propose three hypotheses.

The first hypothesis involves inflammation and the possible formation of neutralizing anti-therapeutic antibodies (ATA). Sarcomas in the present analysis included metastatic osteosarcomas, metastatic soft tissue sarcomas, and other refractory sarcomas. These sarcomas are highly inflammatory and may be associated with the formation of ATA, which can result in an increase in mAb CL. Co-administration of immunosuppressants has been shown to decrease mAb CL [30, 31], and one of the mechanisms has been proposed to be downregulation of the immune response to mAbs and/or reticuloendothelial system-mediated CL [29, 32, 33].

The second hypothesis concerns overall health status. Sarcomas are highly inflammatory and therefore may be associated with worse health status and therefore higher CL of mAbs. Inflammatory markers have been shown to correlate with some clinical variables known to have an important prognostic role (stage, histological subtype, and response to therapy) in soft-tissue sarcoma patients [34, 35]. The percentage of children with primary CNS tumours with albumin below the normal level (35 g l^{-1}) appeared lower than in children with sarcomas: 8% vs. 24%, which supports this hypothesis. However, the significant difference in CL by cancer type still exists after accounting for the effect of albumin, suggesting that some unobserved prognostic factors may play a role [36], such as baseline tumour burden, which has been shown to have a statistically significant and clinically relevant impact on the PK of mAb [37]. However, two factors made it impossible to test tumour burden as a covariate in this analysis. First, tumour response criteria were inconsistent across these studies, which were conducted across a time span of over 12 years. Several different versions of the

Response Evaluation Criteria in Solid Tumors (RECIST) and other criteria (e.g. the Macdonald criteria for glioblastoma) were used. Second, the methods used to measure tumour burden, such as computed tomography scans and magnetic resonance imaging, were inconsistent across studies. However, tumour burden is an indicator of disease burden and health status, which could already be represented by albumin in the model. In addition, the inclusion of tumour burden in the model would limit the applicability of the model to future data owing to the continuous advancement in tumour response criteria and measurement methods.

The third hypothesis concerns concomitant medications. It is possible that children with primary CNS tumours received higher doses of steroids than children with sarcomas. However, a possible effect of steroids on bevacizumab PK has not been reported. Many bevacizumab studies have been conducted in adults, and there has been no observation of any impact of concomitant chemotherapeutic agents on its PK (unpublished data). Further research is warranted in this area. Other factors that showed a statistically significant impact on bevacizumab PK are similar between paediatric and adult cancer patients: CL and V1 increased with BWT and were lower in females, and CL decreased with albumin.

We demonstrated that CL and V1 change very little across ages in paediatric cancer patients after taking into account BWT (Figure 1), indicating that the potential change in PK across ages is mainly caused by the change in body size, and there may be no need to adjust the dose of bevacizumab by age if it is properly dosed by body size.

An important consideration in paediatric oncology drug development is to match the paediatric exposure with the adult exposure because the adult exposure has been well studied for efficacy and safety in relatively large populations. Our results support that the BWT-based dose of bevacizumab is the most appropriate and practical dosing strategy for paediatric patients. First, our results demonstrated that BSA-, IBW-, and tier-based doses offered no substantial advantage over the BWT-based dose (Figure 5). The bevacizumab steady-state Cmin in paediatric patients generally falls within the 90% PI of adult Cmin under all dosing strategies. Clinically meaningful underexposure under the BWT-based dose seems unlikely because Cmin under the BWT-based dose falls below the 90% PI of adult Cmin in only 4% of paediatric patients with a low BWT, and the magnitude of underexposure in this latter group is limited. Second, the BWT-based dose may be associated with fewer safety concerns. Under the BWT-based dose, Cmax is substantially (in 33% of the paediatric patients) below the lower boundary of the 90% PI of adult Cmax. However, under the tier-based dose, Cmax (in 12% of the paediatric patients) exceeded the upper boundary of the 90% PI of adult Cmax. Furthermore, when converted to the mg kg^{-1} dose, the BSA- and tier-based doses exceeded the bevacizumab MTD of 15 mg kg^{-1} previously determined in adults. Finally,

from a practical perspective, BSA-, IBW-, and tier-based doses all require the calculation of BSA and IBW using a certain formula, or a decision to be made on a fixed dose by age or body size range, which could add additional complexity, human errors, and inconsistency. For example, different formulas are available for calculating BSA [38–41], drug preparation and administration may become more inconvenient, and risk of medication errors may occur [42].

Based on simulations, the bevacizumab dose can stay the same for children with primary CNS tumours and those with sarcomas, in spite of the difference in bevacizumab PK by tumour type. In children with all tumour types, the bevacizumab steady-state Cmin falls within the 90% PI of adult Cmin under all dosing strategies, and Cmax does not exceed the upper boundary of the 90% PI of adult Cmax under BWT-based, BSA-based and IBW-based doses.

In conclusion, a robust bevacizumab population PK model for paediatric cancer patients, which can be used for simulations, was developed and externally validated. Children with primary CNS tumours showed significantly lower CL and V1 and higher steady-state exposure than children with sarcomas, but the same dose can be used in children with both tumour types. The BWT-based bevacizumab dose currently used in adults is most appropriate and practical for paediatric cancer patients. Given the similarity in PK among many mAbs [29], this may help to develop the most appropriate and practical paediatric dosing guidelines for other therapeutic mAbs.

Competing Interest

Contributors

All authors contributed substantially to the conception and design of the analysis, drafting or revising the paper, as well as giving final approval for submission.

REFERENCES

1 Ferrara N, Gerber HP, LeCouter J. The biology of VEGF and its receptors. Nat Med 2003; 9: 669–76.

2 Hurwitz H, Fehrenbacher L, Novotny W, Cartwright T, Hainsworth J, Heim W, Berlin J, Baron A, Griffing S, Holmgren E, Ferrara N, Fyfe G, Rogers B, Ross R, Kabbinavar F. Bevacizumab plus irinotecan, fluorouracil, and leucovorin for metastatic colorectal cancer. N Engl J Med 2004; 350: 2335–42.

3 Giantonio BJ, Catalano PJ, Meropol NJ, O'Dwyer PJ, Mitchell EP, Alberts SR, Schwartz MA, Benson AB 3rd. Eastern Cooperative Oncology Group Study E3200. Bevacizumab in combination with oxaliplatin, fluorouracil, and leucovorin (FOLFOX4) for previously treated metastatic colorectal cancer: results from the Eastern Cooperative Oncology Group Study E3200. J Clin Oncol 2007; 25: 1539–44.

4 Sandler A, Gray R, Perry MC, Brahmer J, Schiller JH, Dowlati A, Lilenbaum R, Johnson DH. Paclitaxel–carboplatin alone or with bevacizumab for non-small-cell lung cancer. N Engl J Med 2006; 355: 2542–50.

5 Miller K, Wang M, Gralow J, Dickler M, Cobleigh M, Perez EA, Shenkier T, Cella D, Davidson NE. Paclitaxel plus bevacizumab versus paclitaxel alone for metastatic breast cancer. N Engl J Med 2007; 357: 2666–76.

6 Escudier B, Bellmunt J, Négrier S, Bajetta E, Melichar B, Bracarda S, Ravaud A, Golding S, Jethwa S, Sneller V. Phase III trial of bevacizumab plus interferon alfa-2a in patients with metastatic renal cell carcinoma (AVOREN): final analysis of overall survival. J Clin Oncol 2010; 28: 2144–50.

7 Tewari KS, Sill MW, Long HJ 3rd, Penson RT, Huang H, Ramondetta LM, Landrum LM, Oaknin A, Reid TJ, Leitao MM, Michael HE, Monk BJ. Improved survival with bevacizumab in advanced cervical cancer. N Engl J Med 2014; 370: 734–43.

8 Pujade-Lauraine E, Hilpert F, Weber B, Reuss A, Poveda A, Kristensen G, Sorio R, Vergote I, Witteveen P, Bamias A, Pereira D, Wimberger P, Oaknin A, Mirza MR, Follana P, Bollag D, Ray-Coquard I. Bevacizumab combined with chemotherapy for platinum-resistant recurrent ovarian cancer: the AURELIA open-label randomized Phase III trial. J Clin Oncol 2014; 32: 1302–8.

9 Edlund H, Melin J, Parra-Guillen ZP, Kloft C. Pharmacokinetics and pharmacokinetic–pharmacodynamic relationships of monoclonal antibodies in children. Clin Pharmacokinet 2015; 54: 35–80.

10 Crawford JD, Terry ME, Rourke GM. Simplification of drug dosage calculation by application of the surface area principle. Pediatrics 1950; 5: 783–90.

11 Ross EL, Jorgensen J, DeWitt PE, Okada C, Porter R, Haemer M, Reiter PD. Comparison of 3 body size descriptors in critically ill obese children and adolescents: implications for medication dosing. J Pediatr Pharmacol Ther 2014; 19: 103–10.

12 Lu JF, Bruno R, Eppler S, Novotny W, Lum B, Gaudreault J. Clinical pharmacokinetics of bevacizumab in patients with solid tumors. Cancer Chemother Pharmacol 2008 Oct; 62: 779–86.

13 Glade Bender JL, Adamson PC, Reid JM, Xu L, Baruchel S, Shaked Y, Kerbel RS, Cooney-Qualter EM, Stempak D, Chen HX, Nelson MD, Krailo MD, Ingle AM, Blaney SM, Kandel JJ, Yamashiro DJ, Study C's OG. Phase I trial and pharmacokinetic study of bevacizumab in pediatric patients with refractory solid tumors: a Children's Oncology Group Study. J Clin Oncol 2008; 26: 399–405.

14 Turner DC, Navid F, Daw NC, Mao S, Wu J, Santana VM, Neel M, Rao B, Willert JR, Loeb DM, Harstead KE, Throm SL, Freeman BB 3rd, Stewart CF. Population pharmacokinetics of bevacizumab in children with osteosarcoma: implications for dosing. Clin Cancer Res 2014; 20: 2783–92.

15 Gururangan S, Fangusaro J, Poussaint TY, McLendon RE, Onar-Thomas A, Wu S, Packer RJ, Banerjee A, Gilbertson RJ, Fahey F, Vajapeyam S, Jakacki R, Gajjar A, Goldman S, Pollack IF, Friedman HS, Boyett JM, Fouladi M, Kun LE. Efficacy of bevacizumab plus irinotecan in children with recurrent low-grade gliomas – a Pediatric Brain Tumor Consortium study. Neuro Oncol 2014; 16: 310–7.

16 Beal S, Sheiner LB, Boeckmann A, Bauer RJ. NONMEM User's Guides (1989–2009). Ellicott City, MD, USA: Icon Development Solutions, 2009.

17 Lindbom L, Ribbing J, Jonsson EN. Perl-speaks-NONMEM (PsN) – a Perl module for NONMEM related programming. Comput Methods Programs Biomed 2004; 75: 85–94.

18 R Core Team (2015). R: a language and environment for statistical computing. R Foundation for Statistical Computing, Vienna, Austria. [online] Available at: http://www.R-project.org/ (last accessed Aug 15, 2015).

19 Dong JQ, Salinger DH, Endres CJ, Gibbs JP, Hsu CP, Stouch BJ, Hurh E, Gibbs MA. Quantitative prediction of human pharmacokinetics for monoclonal antibodies: retrospective analysis of monkey as a single species for first-in-human prediction. Clin Pharmacokinet 2011; 50: 131–42.

20 Karlsson MO, Savic RM. Diagnosing model diagnostics. Clin Pharmacol Ther 2007; 82: 17–20.

21 US Department of Health and Human Services, Food and Drug Administration, Center for Drug Evaluation and Research (CDER), Center for Biologics Evaluation and Research (CBER). Guidance for industry population pharmacokinetics [online]. Available at http://www.fda.gov/downloads/Drugs/GuidanceComplianceRegulatoryInformation/Guidances/UCM072137.pdf (last accessed Aug 15, 2015).

22 Committee for Medicinal Products for Human Use (CHMP). Guideline on reporting the results of population pharmacokinetic analyses [online]. Doc. ref. CHMP/EWP/185990/06, London. Available at http://www.ema.europa.eu/docs/en_GB/document_library/Scientific_guideline/2009/09/WC500003067.pdf (last accessed Aug 15, 2015).

23 Bergstrand M, Hooker AC, Wallin JE, Karlsson MO. Prediction-corrected visual predictive checks for diagnosing nonlinear mixed-effects models. AAPS J 2011; 13: 143–51.

24 Ette EI. Stability and performance of a population pharmacokinetic model. J Clin Pharmacol 1997; 37: 486–95.

25 Savic RM, Karlsson MO. Importance of shrinkage in empirical Bayes estimates for diagnostics: problems and solutions. AAPS J 2009; 11: 558–69.

26 Ogden CL, Kuczmarski RJ, Flegal KM, Mei Z, Guo S, Wei R, Grummer-Strawn LM, Curtin LR, Roche AF, Johnson CL. Centers for Disease Control and Prevention 2000 growth charts for the United States: improvements to the 1977 National Center for Health Statistics version. Pediatrics 2002; 109: 45–60.

27 Midgley R, Kerr D. Bevacizumab – current status and future directions. Ann Oncol 2005; 16: 999–1004.

28 US. Department of Health and Human Services, Food and Drug Administration, Center for Drug Evaluation and Research (CDER), Center for Biologics Evaluation and Research (CBER). Guidance for industry. The content and format for pediatric use supplements [online]. Available at http://www.fda.gov/downloads/Drugs/GuidanceComplianceRegulatoryInformation/Guidances/ucm071957.pdf (last accessed Aug 15, 2015).

29 Dostalek M, Gardner I, Gurbaxani BM, Rose RH, Chetty M. Pharmacokinetics, pharmacodynamics and physiologically-based pharmacokinetic modelling of monoclonal antibodies. Clin Pharmacokinet 2013; 52: 83–124.

30 Weisman MH, Moreland LW, Furst DE, Weinblatt ME, Keystone EC, Paulus HE, Teoh LS, Velagapudi RB, Noertersheuser PA, Granneman GR, Fischkoff SA, Chartash EK. Efficacy, pharmacokinetic, and safety assessment of adalimumab, a fully human anti-tumor necrosis factor-alpha monoclonal antibody, in adults with rheumatoid arthritis receiving concomitant methotrexate: a pilot study. Clin Ther 2003; 25: 1700–21.

31 Höcker B, Kovarik JM, Daniel V, Opelz G, Fehrenbach H, Holder M, Hoppe B, Hoyer P, Jungraithmayr TC, Köpf-Shakib S, Laube GF, Müller-Wiefel DE, Offner G, Plank C, Schröder M, Weber LT, Zimmerhackl LB, Tönshoff B. Pharmacokinetics and immunodynamics of basiliximab in pediatric renal transplant recipients on mycophenolate mofetil comedication. Transplantation 2008; 86: 1234–40.

32 Maini RN, Breedveld FC, Kalden JR, Smolen JS, Davis D, Macfarlane JD, Antoni C, Leeb B, Elliott MJ, Woody JN, Schaible TF, Feldmann M. Therapeutic efficacy of multiple intravenous infusions of anti-tumor necrosis factor alpha monoclonal antibody combined with low-dose weekly methotrexate in rheumatoid arthritis. Arthritis Rheum 1998; 41: 1552–63.

33 Ordás I, Mould DR, Feagan BG, Sandborn WJ. Anti-TNF monoclonal antibodies in inflammatory bowel disease: pharmacokinetics-based dosing paradigms. Clin Pharmacol Ther 2012; 91: 635–46.

34 Bien E, Rapala M, Krawczyk M, Balcerska A. The serum levels of soluble interleukin-2 receptor alpha and lactate dehydrogenase but not of B2-microglobulin correlate with selected clinico-pathological prognostic factors and response to therapy in childhood soft tissue sarcomas. J Cancer Res Clin Oncol 2010; 136: 293–305.

35 Bien E, Krawczyk M, Izycka-Swieszewska E, Trzonkowski P, Kazanowska B, Adamkiewicz-Drozynska E, Balcerska A. Serum IL-10 and IL-12 levels reflect the response to chemotherapy but are influenced by G-CSF therapy and sepsis in children with soft tissue sarcomas. Postepy Hig Med Dosw (Online) 2013; 67: 517–28.

36 Yang J, Zhao H, Garnett C, Rahman A, Gobburu JV, Pierce W, Schechter G, Summers J, Keegan P, Booth B, Wang Y. The combination of exposure-response and case–control analyses in regulatory decision making. J Clin Pharmacol 2013; 53: 160–6.

37 Keizer RJ, Huitema AD, Schellens JH, Beijnen JH. Clinical pharmacokinetics of therapeutic monoclonal antibodies. Clin Pharmacokinet 2010; 49: 493–507.

38 Jastaniah W, Aseeri M. A cross-sectional study comparing variation in body surface area and chemotherapy dosing in pediatric oncology using two different methods. J Oncol Pharm Pract 2010; 16: 189–93.

39 Mosteller RD. Simplified calculation of body-surface area. N Engl J Med 1987; 317: 1098.

40 Haycock GB, Schwartz GJ, Wisotsky DH. Geometric method for measuring body surface area: a height–weight formula validated in infants, children, and adults. J Pediatr 1978; 93: 62–6.

41 Du Bois D, Du Bois EF. A formula to estimate the approximate surface area if height and weight be known. Arch Intern Med 1916; 17: 863–71.

42 Shi R, Derendorf H. Pediatric dosing and body size in biotherapeutics. Pharmaceutics 2010; 2: 389–418.

Supporting Information

Additional Supporting Information may be found in the online version of this article at the publisher's web-site:

Figure S1

Correlation between weight-adjusted pharmacokinetic (PK) parameters obtained from the bevacizumab base model and patient variables in paediatric cancer patients. The grey line represents the locally weighted scatterplot smoothing (LOESS); the dashed line represents the

typical value. In the boxplots, the black dots and black lines represent the mean and median value in each group, respectively. ALBU, baseline albumin (g l⁻¹); BWT, baseline body weight (kg); CL.KG, weight-adjusted clearance (ml h⁻¹); r, Pearson correlation coefficient; TPRO, baseline total protein (g l⁻¹); V1.KG, weight-adjusted central volume of distribution (ml)

Figure S2
Goodness-of-fit for the final bevacizumab population pharmacokinetic model in paediatric patients. Conc, concentration; IDENT, identity line; IPRED, individual predicted concentration; LOESS, locally weighted scatterplot smoothing; OBS, observed concentration; PRED, population predicted concentration

Figure S3
The BSA-, IBW-, and tier-based dose for each individual paediatric patient, converted to mg kg⁻¹ dose. BSA, body surface area; BWT, total body weight; IBW, ideal body weight; MTD, maximum tolerated dose previously determined in adults

Table S1
Model parameters of base and final adult population pharmacokinetic models in solid tumours